Envelope Tracking Power Supply for Volume-Sensitive Low-Power Applications Based on a Resonant Switched-Capacitor Converter

Alon Cervera, *Student Member, IEEE* and Mor Mordechai Peretz, *Member, IEEE*
The Center for Power Electronics and Mixed-Signal IC, Department of Electrical and Computer Engineering
Ben-Gurion University of the Negev, P.O. Box 653, Beer-Sheva, 8410501 Israel
cervera@bgu.ac.il , and morp@ee.bgu.ac.il
http://www.ee.bgu.ac.il/~pemic

***Abstract*– This paper introduces a new envelope tracking power supply to enhance the performance and reduce the overall volume of transmitter modules. The realization is based on a gyrator resonant switched-capacitor converter (GRSCC) that acts as a controlled bi-directional current source with a virtually instantaneous response to create the desired envelope. A quasi-non-casual control method is further applied to closely track high-rate signals without further increasing the switching frequency. The resultant dynamic performance for a given envelope reference signal is significantly improved, providing envelope supply voltage without clipping distortion. Design example and simulations are detailed, and the operation of envelope tracker is verified on a 150mW prototype switched at 2.3MHz, able to track a 1MHz envelope with less than half the losses of a linear regulator.**

I. INTRODUCTION

With the proliferation of portable electronics, the issue of power management has become one of the primary factors to achieve small and light equipment, and in particular prolonging the device operability (battery life) and maintaining satisfactory performance. The two main power consumers of a portable system are the processor and the communication (wireless) transmitter. The main objective of the processor's supply is to sustain a well-regulated constant output voltage under wide range of load changes. On the other hand, the main challenge in the design of the transmitter supply is for its voltage to be modulated at base-band signal rate (10MHz range), requiring extremely high control bandwidth [1-4]. Therefore, design efforts are not as much in efficiency but in size of passive components [1].

Envelope Elimination and Restoration (EER) or Envelope Tracking (ET) methods [2-16] realize envelope modulation of the power supply by either linear regulators, switch-mode regulators, or both. To achieve high efficiency of the switched-mode converter, switched-inductor converter topologies are prominent. Ideally there, the efficiency characteristics can be maintained high for wide range of conversion ratios. However, to minimize the necessity of additional linear regulation to achieve the required bandwidth, ultra-fast switching converters are used [16-18] where their switching losses may affect the efficiency. In addition, the total size of these solutions is not necessarily reduced since now inductors are required, which may also prohibit on-chip integration.

Switched-capacitor (SC) technology has a unique benefit of being a 'perfect' candidate for miniaturization and on-chip integration [19-21]. In the context of ET, SC is a poor solution since it can produce high efficiency in singular conversion ratios [22, 23]. Fortunately, a new family of gyrator resonant switched-capacitor converters (GRSCC) with continuous conversion ratio was recently introduced in [24]. In addition to a wider efficiency-curve, the converter has current sourcing capability and has been shown to respond without delay to line and load variations [19]. These attributes make the GRSCC an attractive candidate for ET applications.

The objective of this study is to introduce a *new rapid adaptive voltage scaling envelope tracking system that is realized by a GRSCC for volume-sensitive low-power applications*. The solution, as detailed in Fig. 1, provides a high-efficiency, *volume-saving* alternative to the conventional switched-inductor approach. Combined with a newly developed non-linear controller, the ET power supply minimizes the

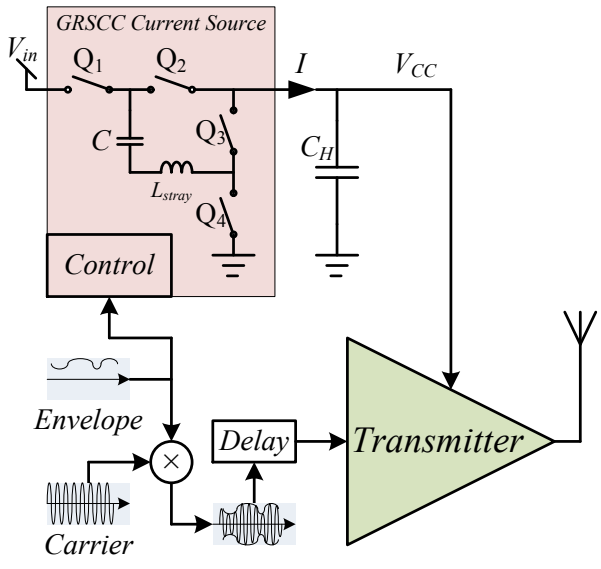

Fig. 1 GRSCC-based envelope tracker.

tracking mismatch and significantly reduces losses related to the linear regulator shape adjuster.

The rest of the paper is organized as follows: Section II describes the new ET principle of operation, portrays the effect of design constraints on the tracking capability, and presents a control scheme to minimize tracking mismatches. Section III delineates the realization of a GRSCC as an envelope tracker. Next, Section IV provides a design example to track a typical orthogonal frequency-division multiplexing (OFDM) RF signal. Experimental results and the conclusion are then provided in Sections V and VI, respectively.

II. Envelope Tracking by Current Sourcing

A generic behavior of the circuit in Fig. 1 can be conceptually described by a controlled current-source that produces $I(t)$ and mimics the operation of the GRSCC, capacitance C_H and a load resistance R_{PA}, as illustrated in Fig. 2. As described in [3,6], a constant resistor is used to emulate the effective loading by a transmitter. For $V_{CC}(t)$ to perfectly match a desired envelope signal $V_E(t)$, the current source is to output a signal $I(t)$ with the linear dependency of the form:

$$I(t) = \frac{V_E(t)}{R_{PA}} + C_H \frac{dV_E(t)}{dt} \quad . \tag{1}$$

A physical converter is limited by current boundaries of I_{min} and I_{max}. As a result, in some cases $V_{CC}(t)$ would be lower than the desired $V_E(t)$, a prohibited scenario in ET applications. Derived from (1) and the circuit in Fig. 2, the response of $V_{CC}(t)$ has a first-order nature due to the current limitation of I_{max}. In most ET applications, the information for the required voltage is available by pseudo non-casual data (e.g. broadcast signal). Therefore, skewing the current injection sequence can be applied by a factor ΔT_{max} which can be expressed as:

$$\Delta T_{max} = -R_{PA} C_H \ln\left(1 - \frac{V_{peak}}{I_{max} R_{PA}}\right), \tag{2}$$

where V_{peak} is the maximum value for V_{CC}(t). A profile vector with length ΔT_{max} of the desired target envelope is used as the reference signal to the tracking system.

To account for the current output limitations and to satisfy $V_{CC}(t) > V_E(t)$ at all times, the reference vector is reconstructed based on the voltage ramp up or down capabilities of the current source. The resulting $V_E^*(t)$ deviates from $V_E(t)$ only when the desired envelope's slews are higher than can be obtained by the current source applied on C_H.

The procedure to generate $V_E^*(t)$ is carried out in three steps and is conceptually illustrated in Fig. 3 which describes an arbitrary portion of a given envelope signal $V_E(t)$. A preliminary step based on the system parameters (i.e., the current ratings, output capacitance and the load), calculates the ramping up/down capabilities in the system as follows:

$$V_{ramp\text{-}up}(t) = I_{max} R_{PA}\left(1 - e^{-\frac{t}{R_{PA} C_H}}\right) \tag{3a}$$

$$V_{ramp\text{-}down}(t) = -I_{max} R_{PA}\left(1 - 2e^{-\frac{t}{R_{PA} C_H}}\right) \quad . \tag{3b}$$

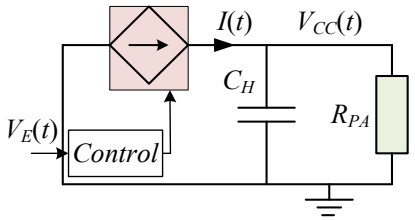

Fig. 2 An average model to illustrate the tracking concept. The GRSCC is modelled by a controlled current source with saturation.

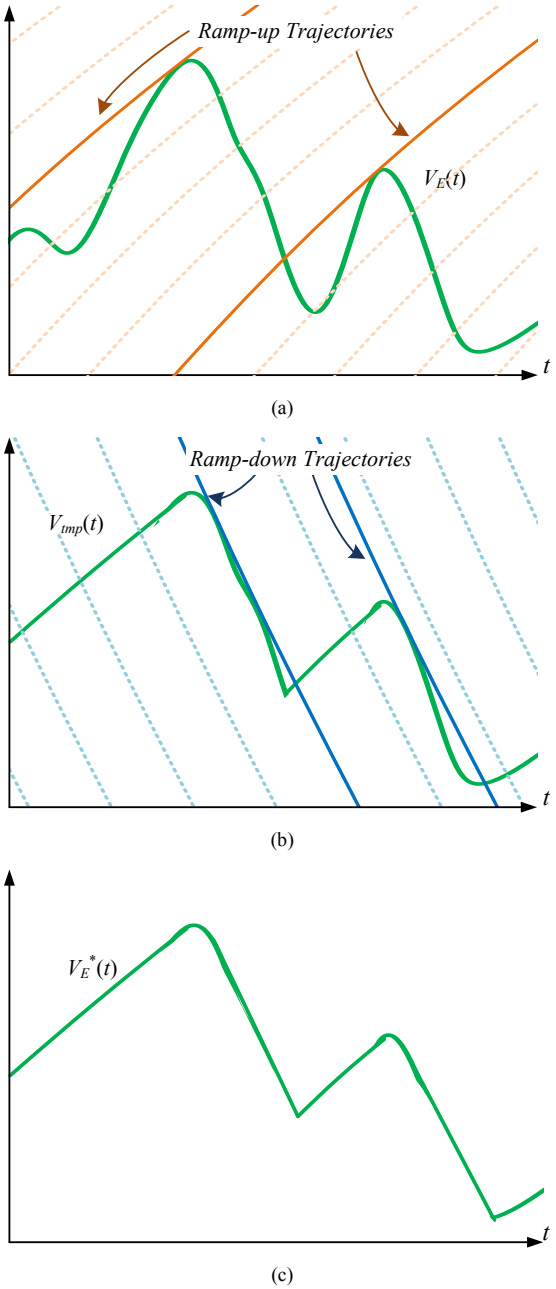

Fig. 3 Step-by-step tracking refernce vector generation procedure. (a) accommodating ramp-up limitations; (b) ramping down; (c) the resultant reference signal compared to the desired one.

In the second step (Fig. 3a), for a given vector length of ΔT_{max}, the possible ramp-up trajectories are compared with the slews of $V_E(t)$ and the reference vector is reconstructed by tangential trajectories to $V_E(t)$ (i.e., with equal slope) to assure that $V_{CC}(t) = V_E^*(t) > V_E(t)$. In the final step (Fig. 3b), the procedure is repeated with the ramp-down trajectories. The resulting reference vector $V_E^*(t)$ is depicted in Fig. 3c. For evaluation purposes, the current-limited injection sequence can be derived using (1) with $V_E^*(t)$. Fig. 4 shows a wider view of the tracking operation, demonstrating generation of a continuous reference vector with severe current output limitations, as well as comparison with constant supply setting. It can be observed that in spite of the limited ramping capabilities, significant portion of the losses is reduced thanks to the tracking method.

III. Realization of a Current Source by a Gyrator Resonant Switched Capacitor Converter

The GRSCC topology (Fig. 1) recently presented in [19] has evolved from the conventional soft-switched resonant switched-capacitor converter (SCC) configuration. As can be seen in Fig. 5, a third switching state is added to balance the charge difference between the input and output rather than introducing losses. By doing so, the converter allows higher efficiency over a wide and continuous step-up/down conversion ratio. Thanks to its soft-switching resonant nature it is applicable at high frequencies and features near-ideal bi-directional pulsed current source behavior. The pulsed behavior can be expressed by average pulse current amplitude, I_{pulse}, of the converter, given by:

$$I_{pulse} = \frac{2CV_{in}}{T_{pulse}} , \qquad (4)$$

where C is the flying capacitor value, V_{in} is the supply voltage, and $T_{pulse} = 3\pi\sqrt{LC}$ is the pulse duration of the converter, set by the resonant network of L and C. Bi-directional operation is realized by reversing the three-state switching scheme, and is expressed in the context of (4) by the expression having positive values for sourcing current and negative values for sinking current operation. As described in detail in [19], immediate response can be achieved with the GRSCC by pulse-density modulation (PDM).

Voltage regulation using ripple-based PDM [19,25] applies valley comparison to the output voltage, i.e. a comparator that triggers the pulsed source each time a reference value is met. Ideally, this method can be applied to envelope tracking by comparing $V_{CC}(t)$ to the synthesized $V_E^*(t)$. Practically, in envelope tracking applications the high-rate envelope variation and, in this study, the need to track a synthesized $V_E^*(t)$ prohibits to use a physical comparator due to the intrinsic delay between the valley detection to the pulse output. To remedy this, pre-calculation and comparison is conducted in advance as follows:

Assuming that the resultant output voltage deviation for a given pulse magnitude of I_{pulse} is relatively small, $V_{CC}(t)$ can be approximated by first order to (Fig. 6):

$$V_{CC}(t) = \begin{cases} \left(I_{pulse} - \frac{V_{CC}(t_0)}{R_{PA}} \right) \frac{(t-t_0)}{C_H} & , \quad t_0 < t < t_1 \\ -\frac{V_{CC}(t_1)}{R_{PA}} \frac{(t-t_1)}{C_H} & , \quad t_1 < t < t_2 \end{cases} , \qquad (5)$$

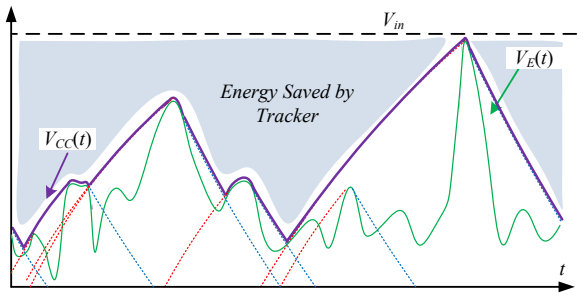

Fig. 4 Illustration describing the tracking operation and saved energy for an information segment in $V_E(t)$ under severe current limitation conditions.

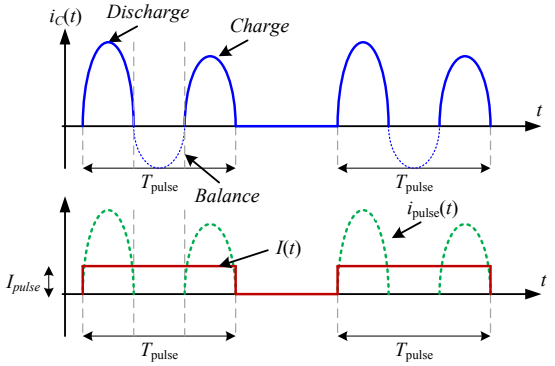

Fig. 5 Current wavforms on the GRSCC depicted in Fig.1 for two pulses. The top graph displays the current on the resonant tank, $i_c(t)$, bottom graph displays the resonant pulse as seen by thhe output, namely $i_{pulse}(t)$ and its' average representation of $I(t)$. switch activity is as follows: discharge - Q_2,Q_4; balance - Q_2,Q_3; charge - Q_1,Q_3.

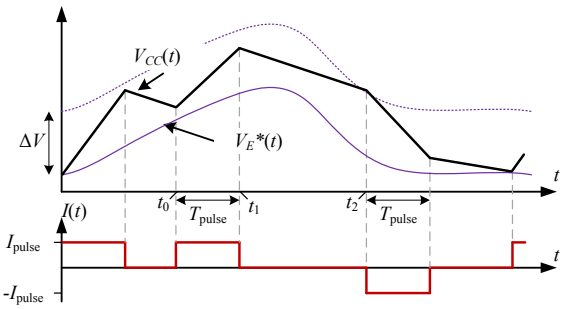

Fig. 6 The methodology for using a constant-pulse source for tracking $V_E^*(t)$

where t_0 is the time of an initiated pulse, $t_1 = t_0 + T_{pulse}$ is the pulse end and t_2 is the trigger point for the next pulse, when $V_{CC}(t) = V_E^*(t)$ (see Fig. 6). $V_{CC}(t)$ is actively reduced when needed by sinking excess charge back to the source using indication from an upper threshold. This threshold is set to $V_{CC}(t) = V_E^*(t) + \Delta V_{CC}$, where ΔV_{CC} is the impact of a single pulse, expressed as:

$$\Delta V_{CC} = \frac{T_{pulse} I_{pulse}}{C_H} . \qquad (6)$$

It should be noted that one potential drawback of this method is lack of feedback and as a result, sensitivity to parameter

variations. This is resolved by either parameter estimation, or worst-case based design with minor effect on the tracking capability.

IV. Simulation Case Study

General design guidelines for the construction of the GRSCC have been previously delineated in [19]. Therefore only specific considerations for the ET application are described through a simulation example.

The target parameters for the envelope tracker are listed in Table I. Given the output power and peak to average power ratio (PAPR), the peak current is $I_{peak} \approx 0.45$ A at $V_{CC} \approx 2.24$ V. Based on (4), the converter is designed to output current of $I_{pulse} = 1$ A to satisfy ramping capabilities of 2 V/μs. The maximum effective frequency is set at $F_{max} = 1/T_{pulse} = 10$ MHz. The resulting resonant network components' values are $C_f \approx 15$ nF, $L \approx 8$ nH. Choosing $C_H = 0.4$ μF results in $\Delta V_{CC} \approx 0.25$ V.

TABLE I – Example Design Specifications

Component	*Value*
Input voltage V_{in}	3.3 V
Minimum input voltage $V_{in,min}$	3 V
Average PA output power P_{out}	250 mW
Reflected load impedance R_{PA}	4.7 Ω
Peak average power ratio PAPR	4
Estimated envelope frequency	2.5 MHz

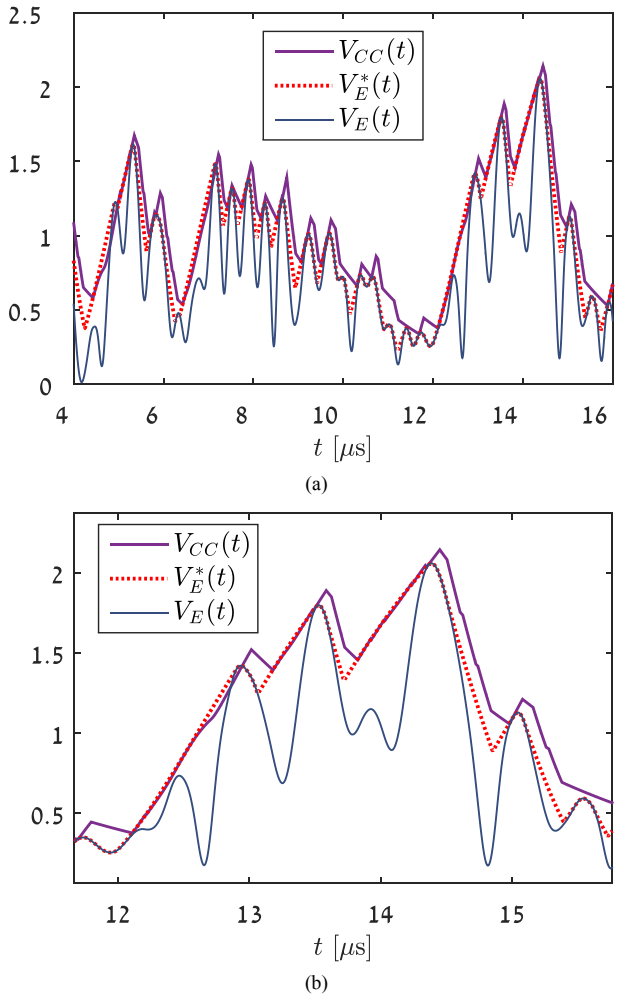

Fig. 7 Simulation results of the converter tracking a reconstructed envelope above $V_E(t)$. (a) wide view, (b) zoom.

The tracking results have been produced using MATLAB and are shown in Fig. 6, which also shows the reference vector generated as described earlier. The design example results in 250% tracking efficiency improvement compared to a constant supply voltage ($\eta_{ET} = V_E / V_{CC} = 70\%$ versus 24%). It should be noted that the efficiency estimation included conservative design of the GRSCC with series loop resistances of $R_S = 50$mΩ, and power-stage efficiency of $\eta = 85\%$.

V. Experimental Results

To verify the operation of the envelope tracker and demonstrate the control scheme solution, a 250mW prototype was built and tested, and is depicted in Fig. 7. Table I lists the power-stage specifications and components' values. The converter was realized by a GRSCC as described in Section III with the resonant tank constructed using capacitors alone. To complete the resonant tank, air-core inductance of 10nH was added to reach the total of 20nH. The envelope reference signal was synthesized using MATLAB, based on generic OFDM symbols, and then translated to pulse timing and direction vectors. GRSCC control was implemented on an Altera Cyclone IV FPGA [26] to create timed source/sink gate-signals for the transistor drivers. Soft-switching was achieved with pre-calibration of switching timings.

Fig. 8 demonstrates the converter's output, recorded from oscilloscope (Teledyne LeCroy HD4016) and compared to the original envelope and the predicted trace through MATLAB. The tracking results are in very good agreement with the theoretical

TABLE II – Experimental Specifications

Component	*Value*
Input voltage V_{in}	3 V
Average PA output power P_{out}	250 mW
Load impedance R_{PA}	4.7 Ω
Tank capacitance C	60 nF
Estimated tank inductance L	20 nH
Output capacitance C_H	0.6 nF
Estimated loop resistance R_S	0.05 Ω
Maximum switching frequency Fs	3 MHz
Estimated envelope frequency	1 MHz
MOSFET type	SiA436DJ

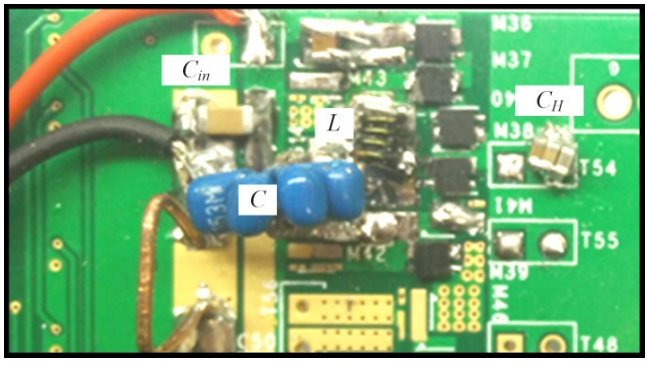

Fig. 8 250 mW 3MHz Experimental prototype. Zoomed in is the resonant tank.

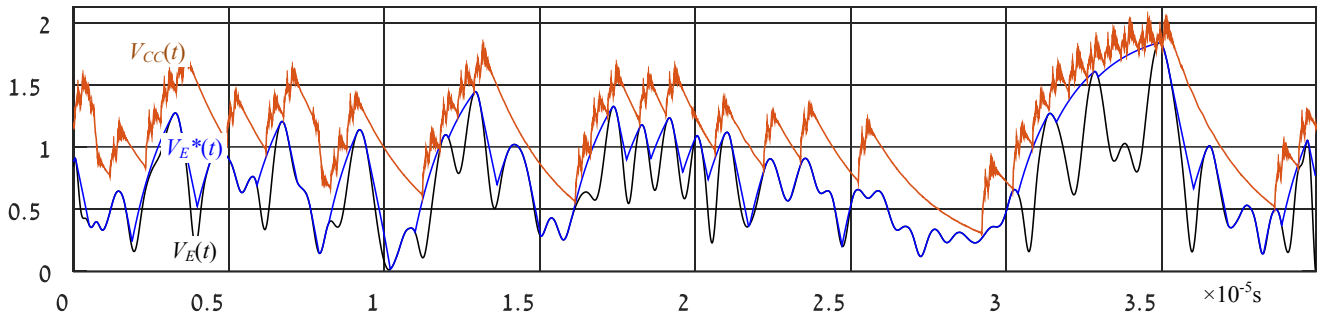

Fig. 9 Experimental results comparing a recorded signal to the original reconstructed envelope and $V_E(t)$.

predictions, verifying the capabilities of the converter as well as the design procedure. The tracking efficiency is measured to be $\eta_{ET} \approx 65\%$ versus 20% in the linear mode approach, with $1/T_{pulse}$ just marginally above the envelope frequency, an improvement of more than 200%. Furthermore, the presented solution is with similar performance to a switched-inductor approach. It should be noted that in some cases the current pulse is triggered before $V_{CC}(t)$ reaches $V_E^*(t)$, and is due to a slight deviation of the resonant parameters and efficiency estimation in relation to the virtual boundaries discussed in Section III.

VI. Conclusion

A new, rapid adaptive voltage scaling envelope tracking system based on a high-efficiency gyrator resonant-switched capacitor converter has been presented. Detailed analysis of the system detailed a new method for envelope tracking by current sourcing which facilitates tight tracking under limited design considerations (e.g. power and switching frequency). A design example has been provided to emphasize considerations oriented toward the target values and performance. The analysis has been methodically verified by simulations and experiments and the results are in excellent agreement with the theoretical predictions providing tracking efficiency improvement of more than 200% using switching frequency of less than 2.5 times higher than the envelope signal.

Combined with the topology benefits, the volume-saving simple GRSCC voltage regulation scheme presents an attractive alternative to the switch-inductor converters, in particular in area sensitive applications, and establishes the foundations for better power delivery concepts for envelope tracking applications.

References

[1] R.Y.L. Zhu, D. Prikhodko, Y. Tkachenko, "LTE power amplifier module design: Challenges and trends," *IEEE International Conference on Solid-State and Integrated Circuit Technology (ICSICT)*, pp.192-195, Nov. 2010.

[2] V. Yousefzadeh, E. Alarcon, D. Maksimovic, "Efficiency optimization in linear-assisted switching power converters for envelope tracking in RF power amplifiers," *IEEE International Symposium on Circuits and Systems, ISCAS 2005*, pp.1302-1305 Vol. 2, May 2005.

[3] V. Yousefzadeh, E. Alarcon, D. Maksimovic, "Band Separation and Efficiency Optimization in Linear-Assisted Switching Power Amplifiers," *IEEE Power Electronics Specialists Conference, PESC '06*, pp.1,7, June 2006

[4] Yusoff, "The auxiliary envelope tracking RF power amplifier system," *PhD diss.,* Cardiff University, 2012.

[5] F. Wang, D. Kimball, J. Popp, A. Yang, D.Y.C. Lie, P. Asbeck, and L. Larson, "Wideband envelope elimination and restoration power amplifier with high efficiency wideband envelope amplifier for WLAN 802.11 g applications," *Microwave Symposium Digest, 2005 IEEE MTT-S International*, pp.345-348, 2005.

[6] M. Vasic, O. Garcia, J.A. Oliver, P. Alou, D. Diaz, J.A. Cobos, "Multilevel Power Supply for High-Efficiency RF Amplifiers," *IEEE Trans. on Power Electronics,* vol.25, no.4, pp.1078-1089, April 2010.

[7] M. Vasic, O. Garcia, J.A. Oliver, P. Alou, J.A. Cobos, "Serial or parallel linear-assisted switching converter as envelope amplifier: Optimization and comparison," *Energy Conversion Congress and Exposition (ECCE), 2011 IEEE* , pp.2488-2494, Sept. 2011.

[8] O. Garcia, M. Vasic, P. Alou, J.A. Oliver, J.A. Cobos, "An overview of fast DC-DC converters for envelope amplifier in RF transmitters," *IEEE Applied Power Electronics Conference and Exposition (APEC)*, pp.1313-1318, Feb. 2012.

[9] A. Soto, J.A. Oliver, J.A. Cobos, J. Cezon, F. Arevalo, "Power supply for a radio transmitter with modulated supply voltage," *IEEE Applied Power Electronics Conference and Exposition,. APEC '04*, pp.392-398, 2004.

[10] J. T. Stauth, "Energy Efficient Wireless Transmitters: Polar and Direct-Digital Modulation Architectures," ProQuest, 2008.

[11] P. Markowski, J. Ronnie, A. Stiedl, "New Achievements in Envelope Tracking Technology," Emerson Network Power, September 2011.

[12] V. Yousefzadeh, E. Alarcon, D. Maksimovic, "Three-level buck converter for envelope tracking applications," *IEEE Trans. on Power Electronics,* vol.21, no.2, pp.549,552, March 2006.

[13] N. Wang, V. Yousefzadeh, D. Maksimovic, S. Pajic, Z.B. Popovic, "60% efficient 10-GHz power amplifier with dynamic drain bias control," *IEEE Trans. on Microwave Theory and Techniques,* vol.52, no.3, pp.1077-1081, March 2004.

[14] M. Norris, D. Maksimovic, "10 MHz large signal bandwidth, 95% efficient power supply for 3G-4G cell phone base stations," *IEEE Applied Power Electronics Conference and Exposition (APEC)*, pp.7-13, Feb. 2012.

[15] F. Wang, D.F. Kimball, J.D. Popp, A.H. Yang, D.Y. Lie, P.M. Asbeck, L.E. Larson, "An Improved Power-Added Efficiency 19-dBm Hybrid Envelope Elimination and Restoration Power Amplifier for 802.11g WLAN Applications," *IEEE Trans. on Microwave Theory and Techniques*, vol.54, no.12, pp.4086-4099, Dec. 2006.

[16] D. Diaz, O. Garcia, J.A. Oliver, P. Alou, Z. Pavlovic, J.A. Cobos, "The Ripple Cancellation Technique Applied to a Synchronous Buck Converter to Achieve a Very High Bandwidth and Very High Efficiency Envelope Amplifier," *IEEE Trans. on Power Electronics*, vol.29, no.6, pp.2892-2902, June 2014.

[17] L. Marco, A. Poveda, E. Alarcon, D. Maksimovic, "Bandwidth limits in PWM switching amplifiers," *IEEE International Symposium on Circuits and Systems (ISCAS 2006) Proceedings*, pp. 5326, May 2006.

[18] K. S. Leung and H. S. H. Chung, "A comparative study of the boundary control of buck converters using first- and second-order switching surfaces—Part I: Continuous conduction mode," *in Proc. IEEE Power Electron. Spec. Conf.,* pp. 2133 -2139, Jun. 2005.

[19] A. Cervera and M.M. Peretz, "Resonant switched-capacitor voltage regulator with ideal transient response," *IEEE Trans. on Power Electronics,* vol.30, no.9, pp.4943-4951, Sep. 2015.

[20] O. Kirshenboim, A. Cervera, and M. M. Peretz, "Improving Loading and Unloading Transient Response of a Voltage Regulator Module Using a

Load-Side Auxiliary Gyrator Circuit," *IEEE Applied Power Electronics Conf., APEC-2015*, pp.913-920, March 2015.
[21] R.C.N. Pilawa-Podgurski and D.J. Perreault, "Merged two-stage power converter with soft charging switched-capacitor stage in 180 nm CMOS," *IEEE Journal of Solid-State Circuits*, vol. 47, no. 7, pp. 1557-1567 2012.
[22] S. Ben-Yaakov, "Behavioral average modeling and equivalent circuit simulation of switched capacitors converters," *IEEE Trans. on Power Electronics,* vol.27, no.2, 632-636, 2012.
[23] S. Ben-Yaakov, "On the influence of switch resistances on switched-capacitor converter losses," *IEEE Trans. on Industrial Electronics, Letters*, vol.59, no.1, 638-640, 2012.
[24] A. Cervera, M. Evzelman, M.M. Peretz, and S. Ben-Yaakov, "A high efficiency resonant switched capacitor converter with continuous conversion ratio," *IEEE Trans. on Power Electronics*, vol.30, no.3, pp.1373-1382, March 2015.
[25] R. Redl and Jian Sun, "Ripple-based control of switching Regulators—An overview," *IEEE Transactions on Power Electronics*, vol. 24, no. 12, pp. 2669-2680 2009.
[26] DE2 Development and Education Board user manual, Altera Corporation, 2006.